Clim Dyn (2016) 46:3337–3350
DOI 10.1007/s00382-015-2772-1

Anthropogenic forcing on the Hadley circulation in CMIP5 simulations

Lijun Tao[1] · Yongyun Hu[1] · Jiping Liu[2]

Received: 3 May 2015 / Accepted: 17 July 2015 / Published online: 30 July 2015

Abstract Poleward expansion of the Hadley circulation has been an important topic in climate change studies in the past few years, and one of the critically important issues is how it is related to anthropogenic forcings. Using simulations from the coupled model intercomparison projection phase 5 (CMIP5), we study influences of anthropogenic forcings on the width and strength of the Hadley circulation. It is found that significant poleward expansion of the Hadley circulation can be reproduced in CMIP5 historical all-forcing simulations although the magnitude of trends is much weaker than observations. Simulations with individual forcings demonstrate that among three major types of anthropogenic forcings, increasing greenhouse gases (GHGs) and stratospheric ozone depletion all cause poleward expansion of the Hadley circulation, whereas anthropogenic aerosols do not have significant influences on the Hadley circulation. Increasing GHGs cause significant poleward expansion in both hemispheres, with the largest widening of the northern cell in boreal autumn. Stratospheric ozone depletion forces significant poleward expansion of the Hadley circulation for the southern cell in austral spring and summer and for the northern cell in boreal spring. In CMIP5 projection simulations for the twenty-first century, the magnitude of poleward expansion of the Hadley circulation increases with GHG forcing. On the other hand, ozone recovery competes with increasing GHGs in determining the width of the Hadley circulation, especially in austral summer. In both historical and projection simulations, the strength of the Hadley circulation shows significant weakening in winter in both hemispheres.

Keywords Hadley circulation · Subtropical dry zone · Increasing greenhouse gases · Ozone depletion and recovery · Anthropogenic aerosols

1 Introduction

Poleward expansion of the Hadley circulation or widening of the tropical belt has been a subject that has drawn intensive studies in the past few years. Independent observational datasets all demonstrated widening of the tropics. The variables include mean meridional mass streamfunctions (Hu and Fu 2007), tropical tropopause heights (Seidel and Randel 2007; Lu et al. 2009), stratospheric ozone (Hudson et al. 2006; Hudson 2012), outgoing longwave radiation (OLR) (Hu and Fu 2007; Hu et al. 2011), tropospheric temperature (Fu et al. 2006), subtropical jet streams (Archer and Caldeira 2008), sea-level pressure and precipitation (Hu et al. 2011), and so on. Although these variables showed different magnitudes and seasonality of trends, they all demonstrated systematic and significant widening of the tropical belt. Comparison and reviews of these observational results can be found in Seidel et al. (2008), Stachnik and Schumacher (2011), Davis and Rosenlof (2012), and Lucas et al. (2013). Progresses in studies of the widening of the Hadley circulation and its influences on regional climate changes are assessed in several chapters of the Fifth Assessment Report by the Intergovermental Panel on Climate Change (IPCC-AR5), especially in Chapter 2 (Hartmann et al. 2013) and Chapter 10 (Bindoff et al. 2013).

✉ Yongyun Hu
yyhu@pku.edu.cn

[1] Laboratory for Climate and Ocean-Atmosphere Sciences, Department of Atmospheric and Oceanic Sciences, School of Physics, Peking University, Beijing 100871, China

[2] Department of Atmospheric and Environmental Sciences, University at Albany, State University of New York, Albany, NY 12222, USA

The consequence of widening of the Hadley circulation is poleward shift of subtropical dry zones in both hemispheres. It was shown that Southern-Hemisphere (SH) semi-arid regions have experienced rainfall reduction since the late 1970s, and it was suggested that the rainfall reduction is due to poleward expansion of the SH Hadley cell (Cai et al. 2012; Cai and Cowan 2013; Kang et al. 2011). Fu et al. (2013) observed that the dry season has increased over southern Amazonia since 1979, and they suggested that it is due to poleward shift of the SH subtropical jet stream. Taylor et al. (2012a) found that ecological changes in the southern Caribbean Sea are related to the shift of the inter-tropical convergence zone (ITCZ) which is associated with poleward expansion of the Hadley circulation. Poleward expansion of the Hadley circulation may also cause changes of water vapor into the stratosphere (Gettelman et al. 2011).

One critically important issue is what forced the observed poleward expansion of the Hadley circulation. Although there is not a closed theory on the width of the Hadley circulation, it is generally thought that the meridional extent of the Hadley circulation is limited by eddy activity near the subtropics (see Section 3.4 in Schneider et al. 2010). Using the Coupled Model Intercomparison Program Phase 3 (CMIP3), Lu et al. (2007) showed that projected global greenhouse warming in the twenty-first century would lead to poleward expansion of the Hadley circulation because global greenhouse warming causes increase in mid-latitude dry static stability (decrease in mid-latitude eddy activity). Especially, Lu et al. (2007) found a widening rate of 0.6° latitude per K for global-mean temperature increase. Their conclusions are supported by sensitivity tests of idealized simulations (Frierson et al. 2007; Sun et al. 2013; Tandon et al. 2013). Son et al. (2008, 2009, 2010) accessed reanalysis and simulation datasets and found that severe ozone depletion in the Antarctic stratosphere plays an important role in causing poleward expansion of the SH Hadley cell. In particular, they demonstrated that the influence of Antarctic ozone depletion on the Hadley circulation mainly occurs in austral summer (December-January–February, DJF), which is consistent with the seasonality in observations (Hu and Fu 2007). The result is further confirmed by Polvani et al. (2011b), Kang et al. (2011), and Min and Son (2013), and it is concluded that stratospheric ozone changes are the main driver of SH atmospheric circulations (Polvani et al. 2011a, b). Chen and Held (2007) suggested that both increasing GHGs and stratospheric ozone depletion are responsible for the observed poleward expansion of the Hadley circulation. They showed that tropospheric warming and stratospheric cooling cause enhanced meridional temperature gradients around the mid-latitude tropopause and thus stronger zonal winds. The latter leads to poleward shift of baroclinic waves, so that the Hadley circulation expands poleward. Allen et al. (2012) suggested that anthropogenic aerosols, such as increasing black carbon and tropospheric ozone in Northern-Hemisphere (NH) mid-latitudes, warm the mid-latitude atmosphere and hence push the maximum meridional climatological temperature gradient poleward, so that the subtropical jet stream and the NH Hadley cell expands poleward. They further suggested that increasing GHGs play a relatively minor role in causing poleward expansion of the NH Hadley cell. However, the effect of aerosols on the Hadley circulation still needs to be further investigated, because of large uncertainties of the spatial and temporal evolution of aerosol emissions (e.g., Bond et al. 2007) and model performances in simulating aerosol radiative effects (e.g., Wilcox et al. 2013). Sea surface temperature (SST) warming was also suggested to have important contributions to poleward expansion of the Hadley circulation. While results of the Atmospheric Model Intercomparison Project phase 2 (AMIP2) do not show significant influences of SST on the Hadley circulation (Johanson and Fu 2009), Hu and Zhou (2010) and Hu et al. (2011) carried out AMIP-type simulations with 12 ensemble members and found that observed SST forcing is able to generate significant poleward expansion of the Hadley circulation. Allen et al. (2014) suggested that the Pacific decadal oscillation (PDO) has important impacts on the width of the NH Hadley cell.

The purpose of the present paper is to examine impacts of anthropogenic forcings, such as increasing GHGs, ozone depletion, and anthropogenic aerosols, on the Hadley circulation, using CMIP5 simulation datasets. In addition to study their effects on the width, we will also study their effects on the strength of the Hadley circulation. Our study will mainly focus on historical simulations for the twentieth century. Projection simulations, the so-called Representative Concentration Pathways (RCPs), will also be examined.

2 Data and methods

2.1 CMIP5 datasets and forcings

In this study, we analyze model outputs from CMIP5 simulations. Simulation results from 39 models with all available ensemble members are used. Details of CMIP5 experimental designs are described in Taylor et al. (2012b). Information of models and experiments involved in this study is given in Table 1.

We will first examine historical simulations with all forcings, such as anthropogenic forcings of increasing GHGs, prescribed ozone depletion and recovery, anthropogenic aerosols (e.g., black carbon, organic carbon and sulfate

Table 1 List of CMIP5 models and available simulations used in this study

Num	Models	All	GHG	Oz	AA	RCP2.6	RCP4.5	RCP6.0	RCP8.5
1	ACCESS1-0	1					1		1
2	ACCESS1-3	2					1		1
3	bcc-csm1-1	3	1			1	1	1	1
4	bcc-csm1-1-m	3				1	1	1	1
5	BNU-ESM	1	1			1	1		1
6	CanESM2	5	5		5	5	5		5
7	CCSM4	6	3	2	3	6	6	6	6
8	CESM1-BGC	1					1		1
9	CESM1-CAM5	3				3	3	2	3
10	CESM1-CAM5-1-FV2		2		2				
11	CESM1-WACCM	4				1	1		1
12	CMCC-CESM	1							1
13	CMCC-CM	1					1		1
14	CMCC-CMS	1					1		1
15	CSIRO-Mk3-6-0	10	5		5	10	10	10	10
16	EC-EARTH	2				1	3		3
17	FGOALS-g2	5	1	1	2	1	1		1
18	FGOALS-s2	3				1		1	3
19	FIO-ESM	3				3	3	3	3
20	GFDL-CM3	5			3	1	1	1	1
21	GFDL-ESM2G	1				1	1	1	1
22	GFDL-ESM2M	1	1		1	1	1	1	1
23	GISS-E2-H	6	5	11	5	1	5	1	1
24	GISS-E2-R	6	5	10	5	1	6	1	1
25	HadGEM2-AO	1				1	1	1	1
26	HadGEM2-CC	3					1		3
27	HadGEM2-ES	5	4			4	4	4	3
28	inmcm4	1					1		1
29	IPSL-CM5A-LR	6			1	4	4	1	4
30	IPSL-CM5A-MR	3				1	1	1	1
31	IPSL-CM5B-LR	1					1		1
32	MIROC5	5				3	3	3	3
33	MIROC-ESM	3				1	1	1	1
34	MIROC-ESM-CHEM	1				1	1	1	1
35	MPI-ESM-LR	3				3	3		3
36	MPI-ESM-MR	3				1	3		1
37	MRI-CGCM3	3				1	1	1	1
38	NorESM1-M	3			1	1	1	1	1
39	NorESM1-ME	1				1	1	1	1
	Model ensemble	38	11	4	11	29	36	22	38

Values in the table indicate the number of available ensemble in each type of simulations. The last row gives the numbers of available models in the present paper

aerosols), and natural forcings of volcanic aerosols and solar variations. Then, we analyze effects of three individual forcings on the Hadley circulation, including increasing GHGs (hereafter denoted by GHG-forcing), ozone depletion and recovery (denoted by Ozone-only), and anthropogenic aerosols (denoted by AA-only). Finally, we analyze RCP projection simulations to estimate possible changes of the Hadley circulation in the twenty-first century. The projection simulations are driven by the four RCPs, labeled as RCP2.6, RCP4.5, RCP6.0 and RCP8.5, respectively. Details of the forcings included in CMIP5 can be found in

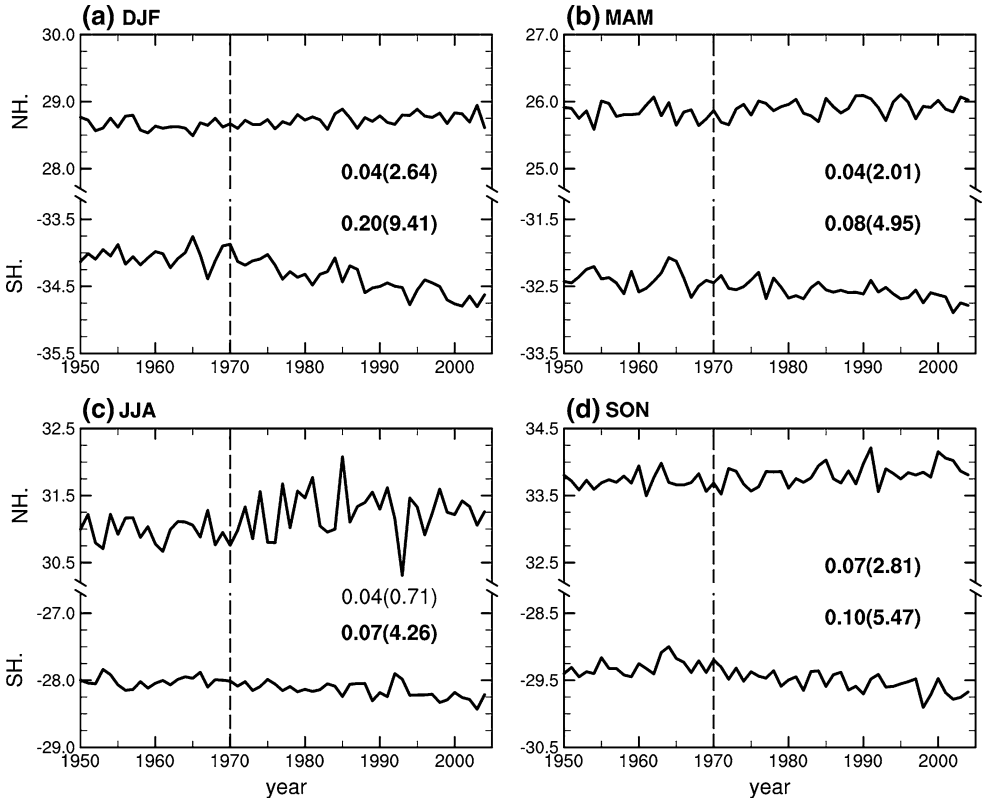

Fig. 1 Time series of multi-model mean poleward-edge latitudes of the Hadley cells for the period of 1950–2005, derived from CMIP5 historical all-forcing simulations. In each plot, time series in the upper part is for the NH cell, while the lower part is for the SH cell. The NH and SH cells are separated by double slashes. In all *plots*, *vertical dash-lines* mark the year of 1970, and values of trends (degree per decade) over 1970–2005 are labeled, and corresponding student's *t* test values are labeled in *brackets*. Trends with statistical significance above the 90 % confidence level (student's *t* test value >1.7) are labeled in *bold*. *Positive trends* indicate poleward shift, while *negative values* indicate equatorward retreat

Moss et al. (2010), Cionni et al. (2011), Lamarque et al. (2011), and Eyring et al. (2013).

2.2 Methods

The Hadley circulation is usually characterized with the mean Meridional Mass Streamfunction (MMS). Following Hu and Fu (2007), the poleward edge of the Hadley circulation is defined as the latitude where MMS at 500 hPa becomes zero in the subtropics. We first calculate poleward-edge latitudes for each model. Then, we calculate multi-model ensemble mean poleward-edge latitudes by averaging the poleward-edge latitudes for all available models. Poleward expansion of the Hadley circulation is derived by calculating linear trends in the multi-model ensemble mean poleward-edge latitudes of the Hadley cells. Statistical significance levels are indicated by student's *t* test values. For historical simulations, trends are calculated over the period of 1970–2005, except for the Ozone-only simulations in which trends are calculated over 1970–2000 because stratospheric ozone begins to increase after 2000. For RCP simulations, we divide the 95-year simulation into two periods: 2006–2040 and 2040–2100. In the first period, ozone recovery is fast, and GHG concentrations keep increasing in all RCPs. In the second period, stratospheric ozone recovery becomes slower, and GHG concentrations decrease for RCP2.6 and remain increasing for RCP4.5, RCP6.0 and RCP8.5 (GHG concentrations become constant after 2070 for RCP4.5). One can also choose either 2030 or 2050 to separate the two periods, but results do not change much. In studying changes in the strength of the Hadley circulation, we use the maximum MMS to represent the Hadley circulation strength.

CMIP5 historical simulations span from 1850 to 2005. Here, all time-series plots are limited over the period of 1950–2005, and all trends are calculated over the period of 1970–2005 for all historical simulations (1970–2000 for the Ozone-only simulations). It is because there are no significant changes in both the width and strength of the Hadley circulation before 1950. In addition, it is worth pointing out that neither pre-industrial control runs nor the natural forcing only runs, which include changes in solar radiation and volcanic aerosols, generate significant changes in the width and strength of the Hadley circulation, consistent with that in Johanson and Fu (2009) and Hu et al. (2013).

3 Results

3.1 Poleward expansion in all-forcing simulations

Figure 1 shows time series of multi-model ensemble mean poleward-edge latitudes of the Hadley cells in historical all-forcing simulations. It indicates systematic and significant

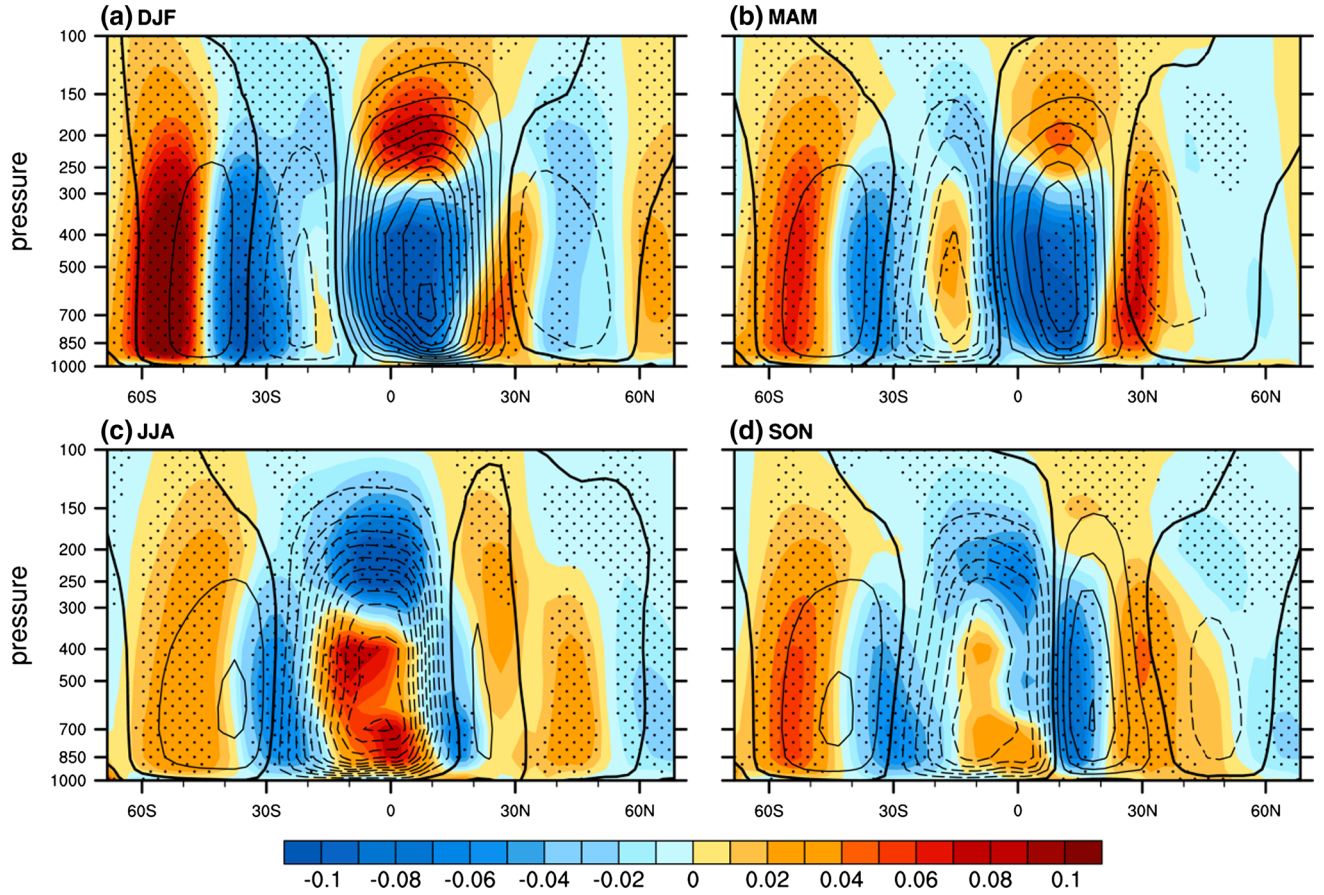

Fig. 2 Seasonal and multi-model mean climatological MMSs (contours) and their trends (color shading) for the period of 1970–2005, derived from CMIP5 historical all-forcing simulations. Clockwise (anti-clockwise) circulations are defined as positive (negative) MMSs, which are denoted with *solid* (*dashed*) *contours*. Contour interval is 5×10^{10} kg s^{-1}. *Thick-solid lines* mark the zero MMS, and the *thick-solid lines* near the subtropics indicate the climatological poleward-edge positions of the Hadley circulation. Positive (negative) MMS trends are indicated by *yellow–red* (*blue*) *color shading*. The trend unit is 1.0×10^{10} kg s^{-1} per decade. Regions marked with *dots* are the areas where statistical significance is above the 90 % confidence level

poleward expansion of both Hadley cells in all seasons, except for boreal summer (June-July–August, JJA) when the trend is less significant. The largest trend is found in austral summer (December-January–February, DJF), with a magnitude of 0.20° per decade (Fig. 1a). As shown below, the largest poleward expansion of the SH cell in DJF is because of severe ozone depletion in the Antarctic stratosphere since the 1970s. For the NH cell, the largest trend is found in boreal autumn (September–October-November, SON), with a magnitude of 0.07° per decade. For the SH cell, significant poleward expansion is found in all seasons, and the trends are greater than that of the NH cell.

The results of all-forcing simulations show consistent seasonality with that in reanalyses. For example, the trend in the NH cell is greater in SON than in other seasons, and the trend in the SH cell is greater in DJF than in other seasons, which are all consistent with results derived from reanalysis (Hu and Fu 2007). However, magnitudes of trends in CMIP5 simulations are much smaller than those in reanalyses, as pointed out by Johanson and Fu (2009). The annual-mean total poleward expansion in historical all-forcing simulations is 0.16° per decade, about 5 times weaker than those in reanalyses, which have trends of 0.5°−1.0° per decade (Hu et al. 2013; Lucas et al. 2013).

Figure 2 shows vertical structures of climatological mean MMSs (contours) and their trends (color shading) over the period of 1970–2005 for historical all-forcing simulations. In general, significant positive (negative) MMS trends are found around the zero-streamlines for both the NH (SH) subtropics, respectively, except for that in the NH subtropics in JJA. The trend patterns indicate poleward expansion of the Hadley circulation in both hemispheres. It is important to note that both the Hadley cells show weakening in the lower and middle troposphere and enhancement in the upper troposphere in all seasons. Since the maximum streamfunction is usually used to characterize the strength of the Hadley circulation, the overlap of weakening MMS trends with the climatological maxima of the

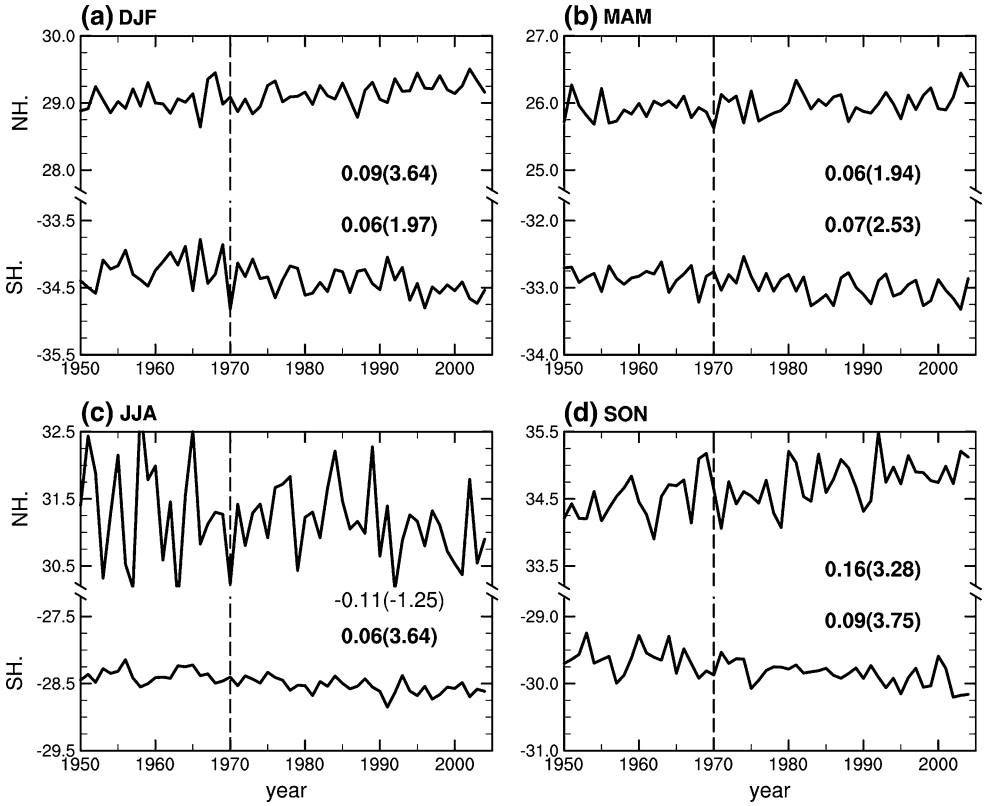

Fig. 3 Same as Fig. 1, except for GHG-forcing simulations

Hadley cells indicates decrease in strength of the Hadley circulation. The enhancement in the upper troposphere is indicative of upward expansion of the Hadley circulation. This is likely a result of increasing tropopause height due to global warming. The spatial patterns of MMS trends also indicate poleward shifts of the Ferrel cells, especially the SH component. Since the Ferrel cells are eddy-driven, the results here suggest poleward shift of baroclinic eddies in all-forcing simulations. We will return to this issue of weakening of the Hadley circulation later.

3.2 Poleward expansion with individual forcings

In this section, we study effects of individual forcings on the Hadley circulation. Figure 3 shows time series of poleward-edge latitudes of the Hadley circulation for historical GHG-forcing simulations. For the NH cell, the largest poleward expansion is in SON, with a magnitude of 0.16° per decade and statistical significance above the 99 % confidence level. Trends in DJF and MAM are also significant, with magnitudes of 0.09 and 0.06° per decade, respectively. Edge-latitudes of the NH cell in JJA demonstrate large interannual fluctuations. Thus, the trend is insignificant. It is noticed that trend magnitudes forced by GHG-forcing alone are nearly twice as large as those by all forcings. One may attribute the difference to different ensemble numbers of models between GHG-forcing and all-forcing simulations. However, results do not change if the same models and ensemble numbers of simulations are used for both GHG-forcing and all-forcing simulations (not shown). The seasonality of poleward expansion of the NH cell is quite similar to that in all-forcing simulations.

The SH cell also shows significant poleward expansion in all the seasons. Trend magnitudes do not vary much with seasons, and they are slightly weaker than those in all forcing simulations, except for that in DJF when GHG-forcing alone generates about one-third of the trend forced by all forcings. As shown below, that is because poleward expansion of the SH cell is largely due to severe ozone depletion in the Antarctic stratosphere.

Figure 4 shows time series of poleward-edge latitudes of the Hadley circulation in Ozone-only simulations. It is important to note that the trends have strong seasonality. For the NH cell, significant poleward expansion of the Hadley circulation is found only in boreal spring (MAM). For the SH cell, significant trends are found only in austral spring (SON) and summer (DJF), and the largest poleward expansion of the SH cell occurs in DJF, with a magnitude of 0.20° per decade. These are the seasons when polar stratospheric ozone depletion has the largest radiative cooling effects on atmospheric thermal structures and circulations. While the effect of Antarctic stratospheric ozone depletion on the SH cell has been greatly emphasized by Son et al. (2008, 2009, 2010) and Polvani et al. (2011b), the effect of

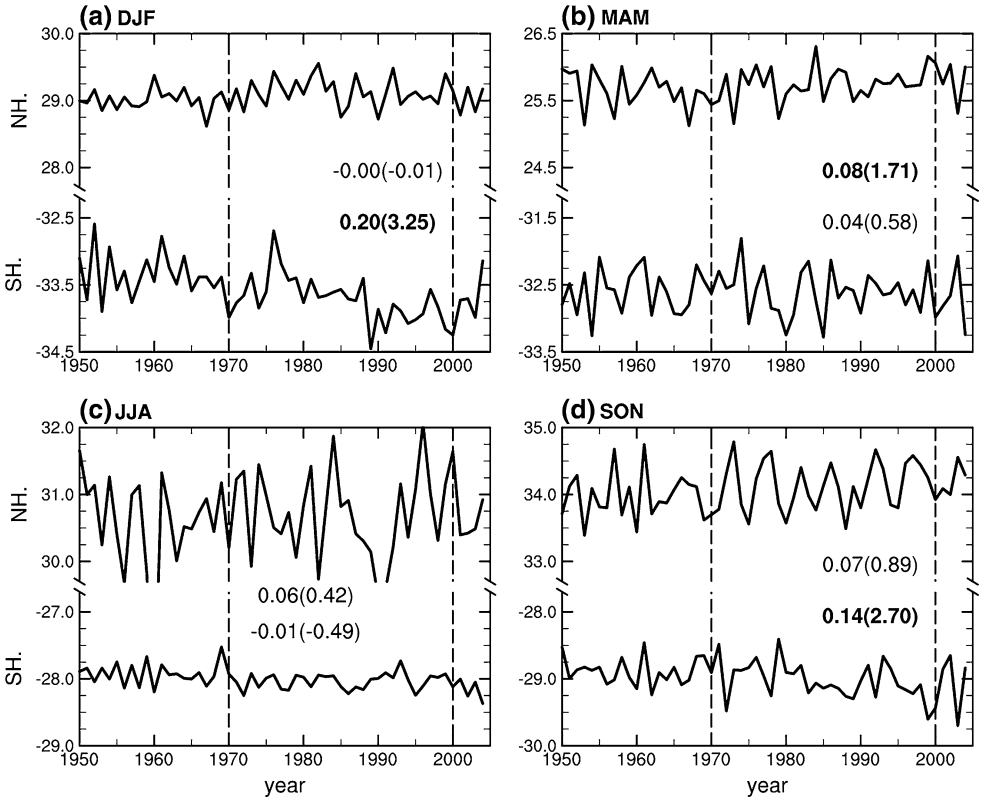

Fig. 4 Same as Fig. 1, except for Ozone-only simulations. Trends labeled in *plots* are calculated over the period of 1970–2000, which are marked by *vertical dashed-lines*

Arctic ozone depletion on the NH cell has not been mentioned before. Here, the CMIP5 Ozone-only simulations indicate that Arctic stratospheric ozone depletion can also cause significant poleward expansion of the Hadley circulation, though stratospheric ozone depletion is weaker in the Arctic than in the Antarctic.

Time series in Fig. 4 demonstrates that the width of the Hadley circulation is rather sensitive to stratospheric ozone changes. That is, ozone depletion causes poleward expansion of the Hadley circulation, whereas ozone recovery causes equatorward retreat. In DJF (Fig. 4a), the poleward edge of the SH cell expands poleward from the 1970s to about 2000. Then, it retreats equatorward over the period of 2000–2005. It is the same for the SH cell in SON and the NH cell in MAM. The timing is coincident with stratospheric ozone changes in both polar regions, which showed stabilizing and even weak increase since the late 1990s.

We also analyzed CMIP5 simulation results of anthropogenic aerosol forcing. It is found that anthropogenic aerosol forcing does not generate significant changes in the width of the Hadley circulation for both hemispheres (not shown). This is not consistent with the results by Allen et al. (2012, 2014). However, it does not necessarily contradict with their results. It is because in CMIP5 simulations anthropogenic aerosols include at least three types of aerosols, such as the black carbons, organic carbons and sulfate aerosols, whereas anthropogenic aerosol forcings considered by Allen et al. (2012, 2014) are absorbing aerosols (e.g., black carbons) and tropospheric ozone. On the other hand, the insignificant effect of anthropogenic aerosols on the Hadley circulation could be due to the inter-model diversity in aerosol burden and cloud sensitivity to aerosols in CMIP5 simulations, as argued by Wilcox et al. (2013).

Figure 5 illustrates seasonal variations of climatological MMSs (contours) and their trends (color shading) at 500 hPa for historical simulations. For all-forcing simulations (Fig. 5a), there is a seasonally varying band of positive and significant MMS trends around the poleward edge of the NH cell. It indicates poleward expansion of the NH Hadley cell. Similarly, a band of negative and significant MMS trends is found around the poleward edge of the SH cell, which indicates poleward expansion of the SH Hadley cell. In addition, negative MMS trends overlap the climatological maxima of the NH cell in boreal winter, indicating weakening of the NH cell. Similarly, positive MMS trends overlap the maxima of the SH cell in austral winter, indicating weakening of the SH cell. Trends in GHG-forcing simulations demonstrate similar spatial–temporal patterns to those in all-forcing simulations (Fig. 5b). It suggests that increasing GHGs are the major forcing in historical all-forcing simulations in causing widening and weakening of the Hadley circulation. For Ozone-only simulations (Fig. 5c), MMS trends show poleward expansion of the Hadley circulation in both hemispheres. However, these

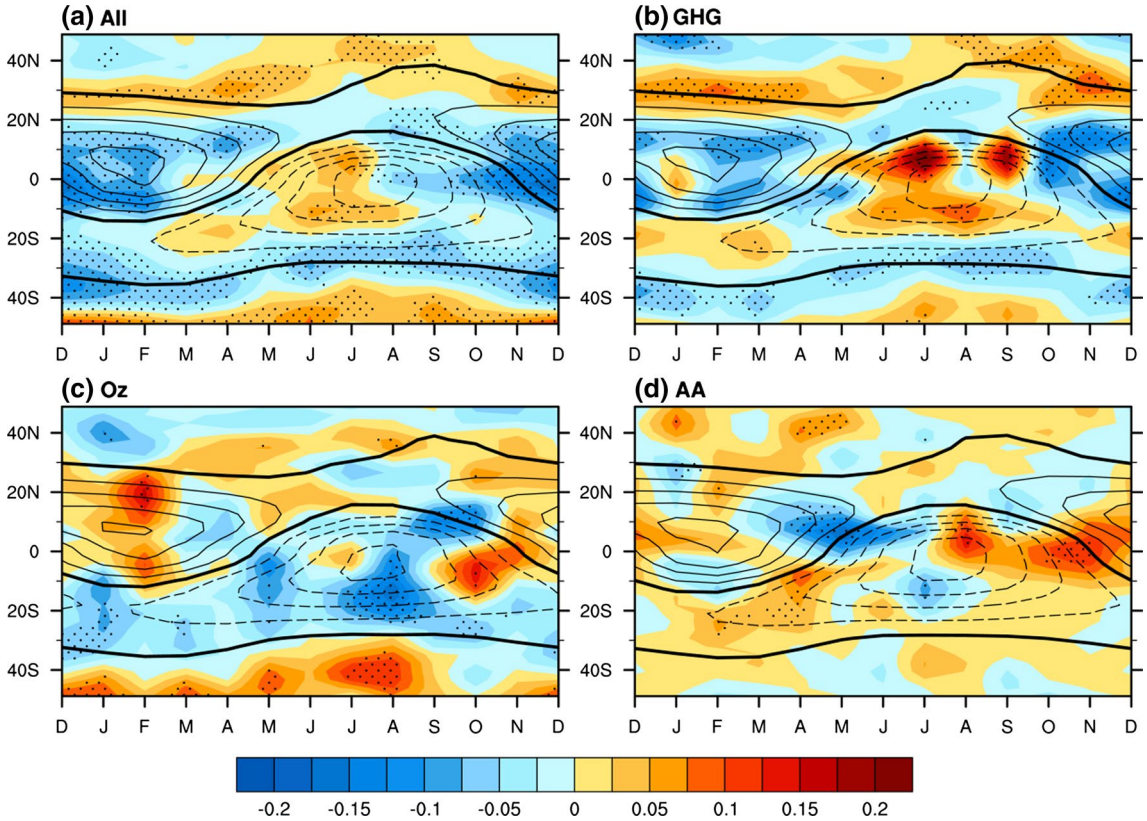

Fig. 5 Latitude-month *plots* of climatological MMSs (contours) and their trends (*color shading*) at 500 hPa over the period of 1970–2005 for **a** All-forcing, **b** GHG-forcing and **d** Anthropogenic aerosols, and over the period of 1970–2000 for **c** Ozone-only. Contour interval is 5.0×10^{10} kg s^{-1}, and the trend unit is 1.0×10^{10} kg s^{-1} per decade. The *thick-solid contours* near the subtropics are the *zero streamlines* and indicate the climatological poleward edges of the Hadley cells. Areas with *dots* are the regions where trends have statistical significance above the 90 % confidence level

trend patterns do not show weakening of the Hadley circulation. Instead, the spatial–temporal patterns of trends indicate strengthening of the Hadley circulation in winter in both hemispheres (less significant at the 90 % confidence level). Comparison of Fig. 5b, c suggests that increasing GHGs and ozone depletion have different influences on the strength of the Hadley circulation, though they both cause poleward expansion. Figure 5d shows seasonal variations of MMS trends in CMIP5 historical simulations with anthropogenic aerosol forcing. As mentioned above, no significant trends in width and strength are found in Fig. 5d.

3.3 Poleward expansion in RCP simulations

Using simulation results from 16 available CMIP5 models, Hu et al. (2013) have shown that the magnitude of poleward expansion of the Hadley circulation increases with RCP forcing for the twenty-first century. Here, we re-examine trends in the width of the Hadley circulation in RCP simulations from 39 models. Figure 6 shows time series of multi-model mean poleward-edge latitudes of the NH cell from RCP simulations. As mentioned in Sect. 2, trends are calculated over two periods: 2006–2040 and 2040–2100. In the first period, trends in SON are the largest and statistically significant for all RCPs (Fig. 6d). In particular, RCP8.5 generates a significant trend of 0.21° per decade. In contrast, trends in JJA are all insignificant. Trends in DJF are significant, except for RCP4.5. In MAM, only RCP8.5 generates a significant trend, while all other three RCPs generate insignificant trends. In the second period, the largest trends are also in SON, except for RCP2.6 that generates a weak negative trend. In JJA, trends for RCP2.6 and RCP4.5 are insignificant, while trends for RCP6.0 and RCP8.5 are somehow negative. In DJF and MAM, RCP2.6 and RCP4.5 generate either negative or insignificant weak trends, while RCP6.0 and RCP8.5 generate significant trends, and these trends are all greater than those in the first period.

Figure 7 shows time series of multi-model mean poleward-edge latitudes of the SH cell. In the first period, positive and significant trends are found for all RCPs in JJA and SON. In MAM, trends are also significant, except

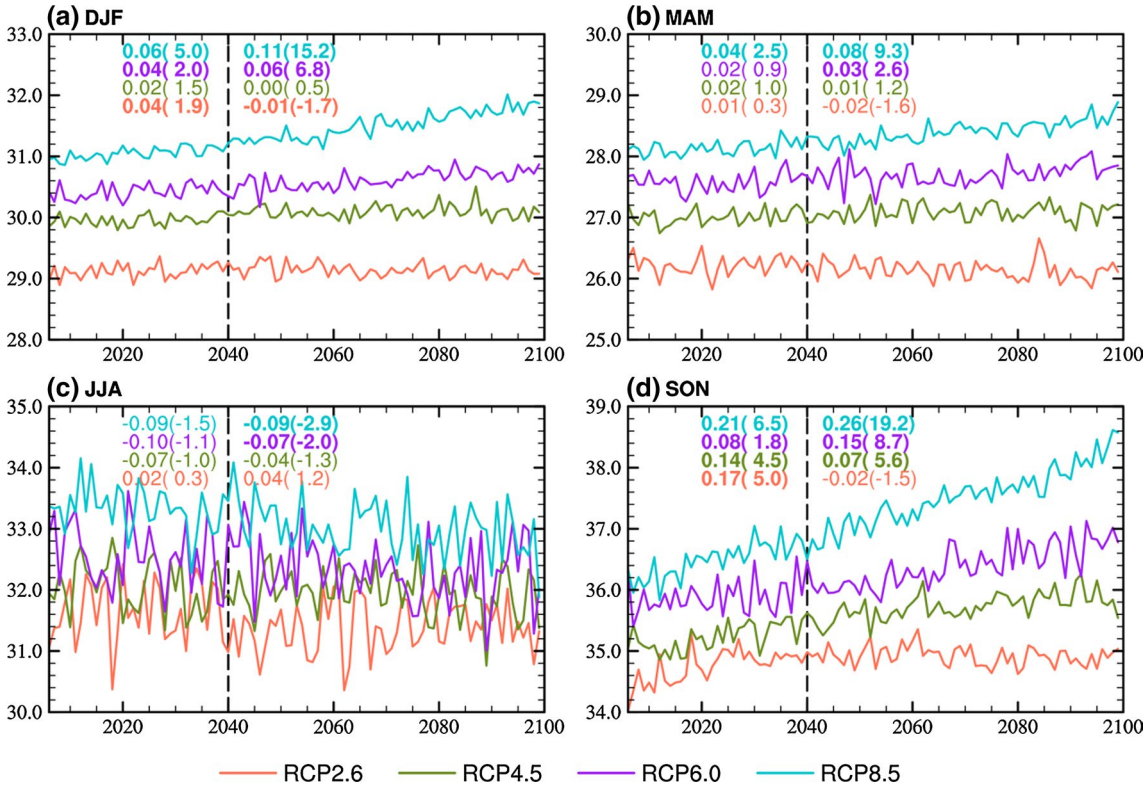

Fig. 6 Time series of multi-model mean poleward-edge latitudes of the NH Hadley cell from RCP simulations. The latter *three lines* are shifted by 1.0°, 1.3°, and 2.1° latitudes to their original positions in order to avoiding overlap. *Vertical dash-lines* correspond to year 2040, which divide the twenty-first century into two periods. Trends and their corresponding student's *t* test values (*in brackets*), are labeled in the *plots*. Trends with significance above the 90 % confidence level (student's *t* test value >1.7) are shown in *bold*. *Positive trends* indicate poleward expansion of the Hadley circulation, while negative trends indicate equatorward retreat

for RCP2.6 that generates a weak insignificant trend. It is important to note that trends in DJF are either insignificant or weaker compared with trends in other three seasons. The weaker trends in DJF are very likely a result of the competition between Antarctic ozone recovery and increasing GHGs. As discussed above, ozone recovery leads to equatorward retreat of the SH Hadley cell, which partly cancels poleward expansion forced by increasing GHGs. In the second period, trends for RCP4.5, RCP6.0, and RCP8.5 are all positive and significant in all seasons, except for RCP4.5 in DJF. However, RCP2.6 generates significant negative trends in DJF, MAM, and JJA. Especially, the negative trend in DJF is as large as 0.04° per decade. The negative trends for RCP2.6 could be caused by two reasons. One is that GHG concentrations of RCP2.6 begin to decrease after 2040. The other one is that Antarctic ozone recovery would lead to equatorward retreat of the SH Hadley cell. If one looks at the time series of RCP2.6 in Fig. 7a carefully, one would find that there is a turning point around 2065. The time series demonstrates systematic equatorward retreat before 2065, with a magnitude of 0.03° per decade (significant at the 99 % confidence level). Then, the time series becomes flat. It is likely that the faster equatorward retreat before 2065 is a result of both Antarctic ozone recovery and decrease of GHG concentrations. It is because in RCP simulations, Antarctic stratospheric ozone will completely recover by the time of 2065 in CMIP5 prescribed ozone (Eyring et al. 2013). After 2065, decrease in GHG alone causes slower equatorward retreat of the poleward edge.

Comparison between the two periods shows that RCP6.0 and RCP8.5 generate greater poleward expansion for both NH and SH Hadley cells in the second period than in the first period. This is because for both RCP6.0 and RCP8.5 GHG concentrations increase faster and become dominant in the second period. For RCP2.6 and RCP4.5, trends in the second period are either weak or negative because of decrease or stabilization of GHG concentrations. In addition, ozone recovery also causes equatorward retreat of the Hadley circulation.

Figure 8 shows latitude-month plots of climatological multi-model mean MMS and trends at 500 hPa for RCP simulations over 2040–2100. The spatial–temporal patterns of MMS trends for RCP6.0 and RCP8.5 are rather similar to those of historical all-forcing and GHG

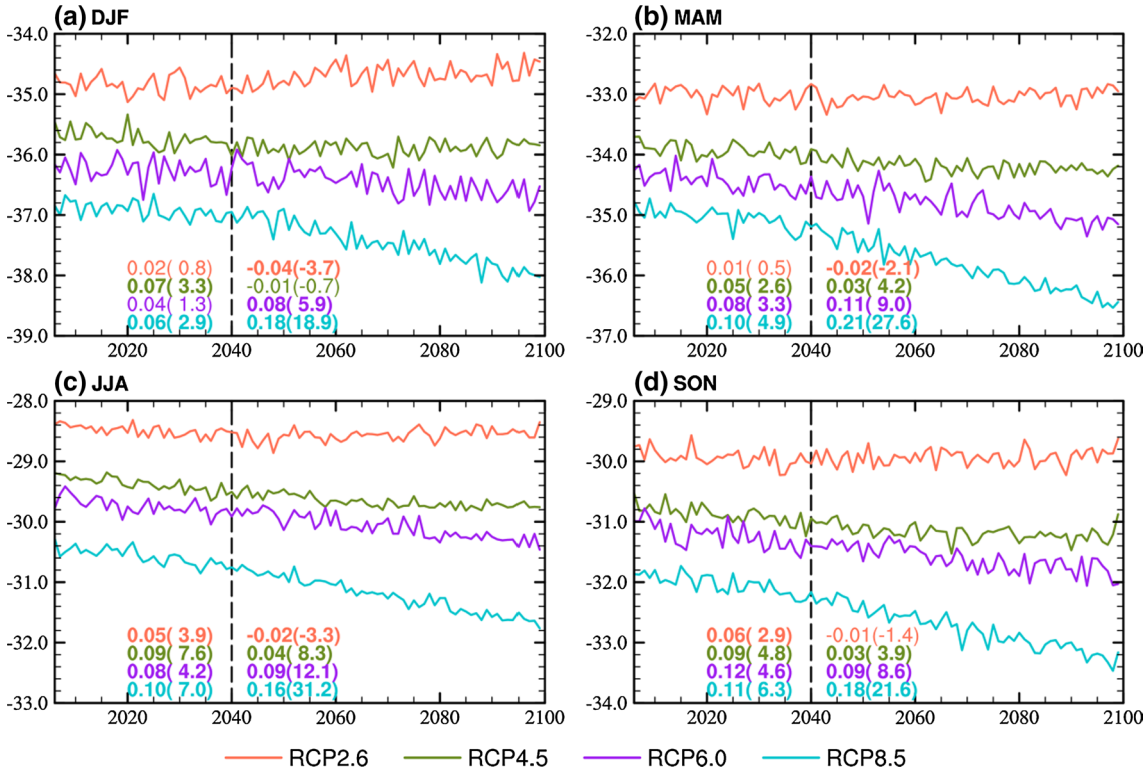

Fig. 7 Same as Fig. 6, except for the SH cell

simulations. The bands of positive and negative trends at the poleward edges of the Hadley cells indicate poleward expansion of the Hadley circulation in NH and SH, respectively. MMS trend patterns also indicate weakening of the Hadley circulation, especially in the winter season in each hemisphere. For RCP8.5, the maximum MMS is reduced by about 10 % over the twenty-first century. RCP4.5 also generates similar spatial–temporal patterns of MMS trends, except for weaker magnitudes. However, RCP2.6 generates nearly opposite spatial–temporal trend patterns to those of stronger RCPs.

To further illustrate changes in the strength of the Hadley circulation, we plot time series of the multi-model mean maximum MMS at 500 hPa for RCP8.5 in Fig. 9. The maximum MMS of the NH cell shows significant weakening trends in all seasons. The largest weakening occurs in DJF, with a value of -0.25×10^{10} kg s^{-1} per decade over the period of 2040–2100. In other word, the maxima of the NH winter cell would be weakened by about 8 % over the 60 years. The smallest weakening is found in JJA, about -0.08×10^{10} kg s^{-1} per decade. The SH cell also shows weakening in DJF, MAM, and JJA. However, it has a weak increase in SON. The largest weakening of the SH cell occurs also in winter season (JJA), about -0.16×10^{10} kg s^{-1} per decade. It is found that weakening trends are much greater in the second period than in the first period. In general, the results here are consistent with that in CMIP3 (Lu et al. 2007), that is, the Hadley circulation is weakened as it expands poleward.

4 Conclusions

We have studied changes in the width and strength of the Hadley circulation in CMIP5 historical and projection simulations. In particular, we have analyzed influences of individual forcings on the Hadley circulation. We use Fig. 10 to summarize trends in the width of the Hadley circulation calculated from CMIP5 historical simulations. For the NH cell, neither natural forcing nor anthropogenic aerosols generate significant trends in the width in all four seasons. GHG-forcing yields significant positive trends in DJF, MAM, and SON, but not in JJA. The largest trend due to GHG-forcing is in SON, about 0.16° per decade. Ozone-only forcing generates a significant positive trend of 0.08° per decade only in boreal spring (MAM). All forcings cause significant positive trends in DJF, MAM, and SON. All trends in JJA are less significant due to large interannual variability. As shown here and pointed out by Johanson and Fu (2009) and Hu et al. (2013), poleward expansion of the Hadley circulation in CMIP5 historical all-forcing simulations is much weaker than observations.

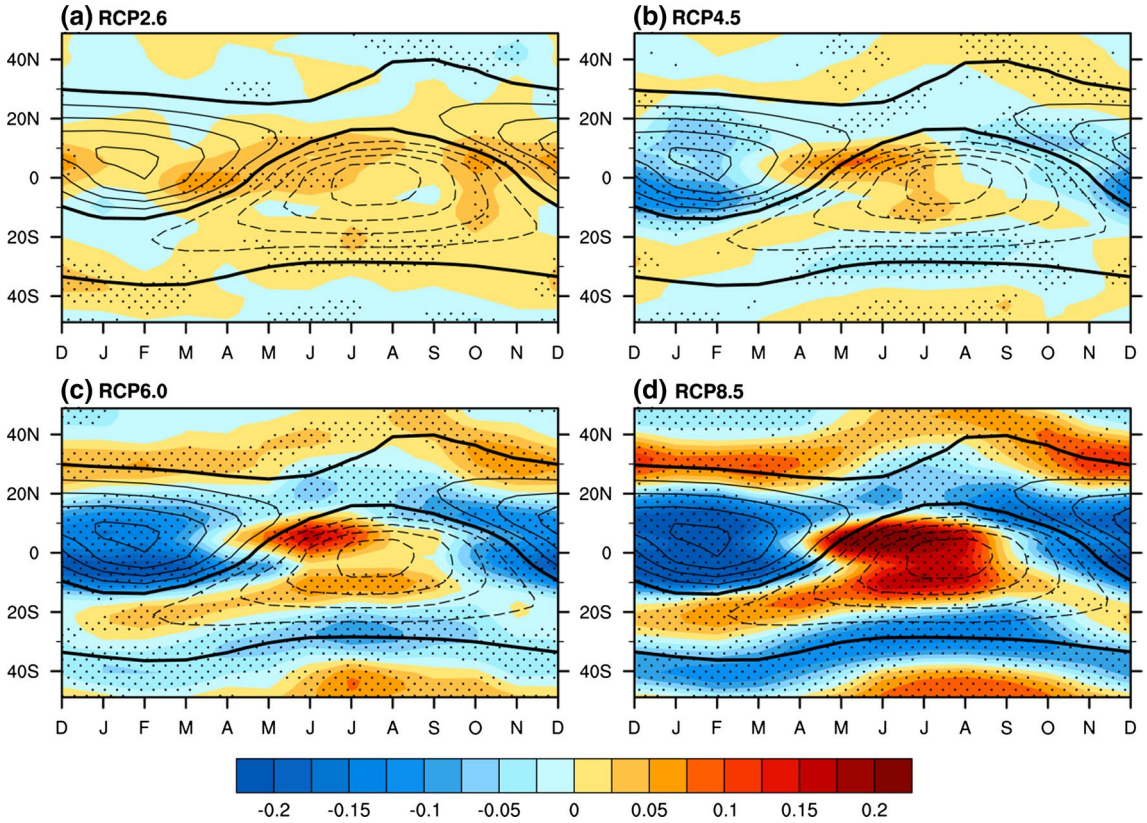

Fig. 8 Same as Fig. 5, except for RCP simulations over the period of 2040–2100. **a** RCP2.6, **b** RCP4.5, **c** RCP6.0, and **d** RCP8.5. The trend unit is 1.0×10^{10} kg s^{-1} per decade

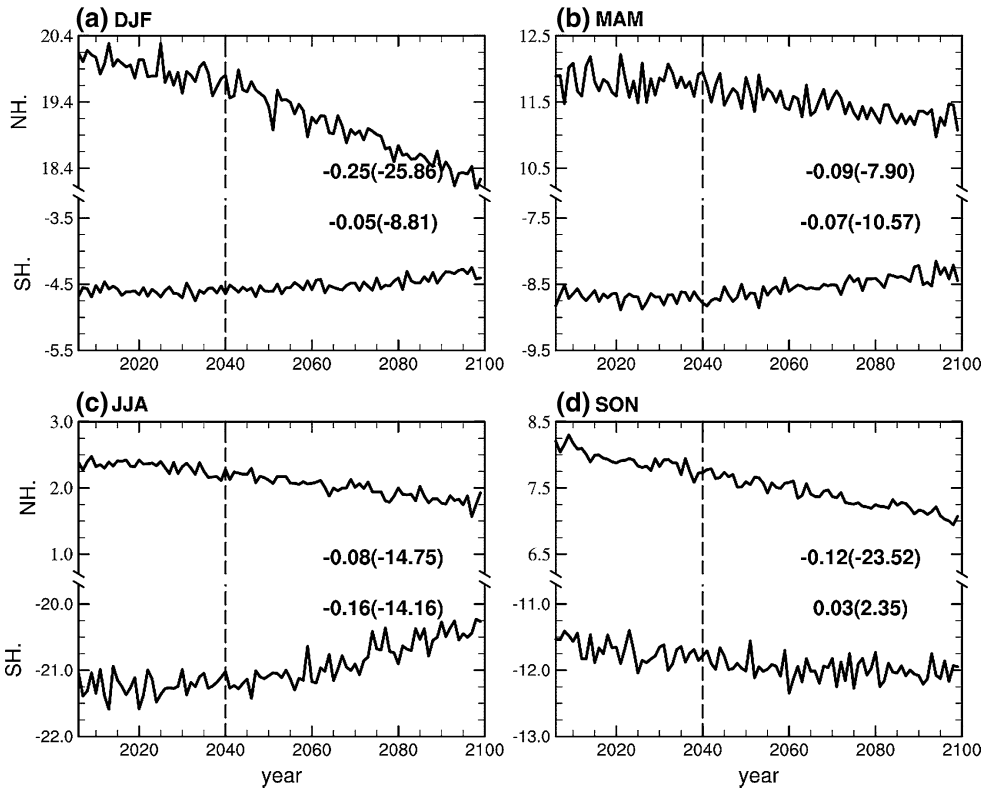

Fig. 9 Time series of the maximum MMS of the Hadley cells, derived from RCP8.5 simulations. **a** DJF, **b** MAM, **c** JJA, and **d** SON. Trends labeled in plots are calculated over the period of 2040–2100. The trend unit is 1.0×10^{10} kg s^{-1} per decade. Digits in *brackets* are student's *t* test values

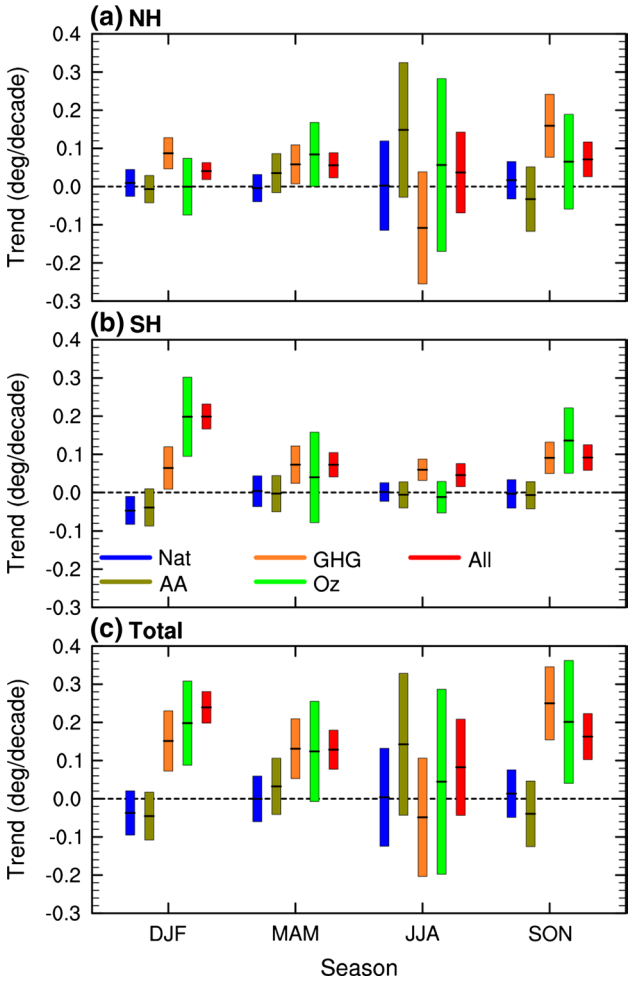

Fig. 10 Seasonal-mean poleward expansion of poleward edges of the Hadley circulation at 500 hPa, derived from CMIP5 historical simulations for the period of 1970–2005 (1970–2000 for Ozone-only). *Positive trends* indicate poleward expansion of the Hadley circulation and *negative values* indicate equatorward retreat. *Error bars* are ±1.7 standard derivations (90 % confidence level). Unit is degree per decade. **a** The NH cell, **b** the SH cell, and **c** total poleward expansion

For the SH cell, neither natural forcing nor anthropogenic aerosols generate significant trends in all seasons, except for DJF in which natural forcing somehow causes a marginally significant negative and weak trend. GHG-forcing causes positive trends in all seasons, and these trends are more seasonally uniform than those in NH. Ozone-only forcing leads to significant positive trends in austral autumn and summer (SON and DJF). The largest trend occurs in DJF, with a magnitude of about 0.2° per decade. All forcings generate significant trends in all seasons. The largest trend occurs in DJF, which has the same magnitude as that of Ozone-only forcing. Total trends (the sum of trends in both hemispheres) are plotted in Fig. 10c. The total trends are relatively large in DJF and SON.

These results in historical simulations indicate that the observed poleward expansion of the Hadley circulation is forced by anthropogenic forcings, such as increasing GHGs and stratospheric ozone depletion, and that natural forcing does not force such changes of the Hadley circulation. GHG-only forcing generates the largest poleward expansion of the NH cell in SON. The Ozone-only forcing causes the relatively largest poleward expansion of the SH cell in DJF. It also generates significant trends in SON and of the NH cell in MAM, but not in other seasons. The seasonality of ozone-induced trends is consistent with observations (Hu and Fu 2007). Especially, Fig. 4 indicates that the width of the Hadley circulation is sensitive to stratospheric ozone changes. In contrast, no significant changes in both width and strength of the Hadley circulation are found in anthropogenic aerosol simulations.

For RCP projection simulations, magnitudes of poleward expansion of the Hadley circulation increase with increasing GHG forcing in general. RCP8.5 forces the greatest poleward expansion of about 0.26° per decade for the NH cell in SON over the period of 2040–2100. By contrast, RCP2.6 produces relatively weak or negative trends over both periods. It appears that the width of the Hadley circulation is very sensitive to GHG forcing. As GHG forcing of RCP2.6 decreases in the second half of the twenty-first century, the Hadley circulation shows equatorward retreat for both NH and SH cells. For RCP4.5, poleward expansion of the Hadley circulation is also smaller in the second period than in the first period because GHG concentrations no longer increase after 2070. Ozone recovery in the twenty-first century has important influences on the width of the Hadley circulation in RCP simulations. For the first period of the twenty-first century, poleward expansion of the SH cell is weaker in DJF than in other seasons in general. It is indicative of cancellation between Antarctic ozone recovery and increasing GHGs in determining the width of the Hadley circulation.

Results in both historical all-forcing simulations and projection simulations indicate that the strength of the Hadley circulation is weakened as its width is widened, especially in the winter season in each hemisphere. For individual forcings, GHG-forcing causes weakening of the Hadley circulation, Ozone-only forcing causes weak strengthening of the Hadley circulation, and anthropogenic aerosol forcing has no significant influences on the strength of the Hadley circulation.

There are three points worth pointing out for future investigations. First, it is not clear why GHG-forcing generates the largest poleward expansion of the NH cell in boreal autumn (SON). Second, while increasing GHGs and stratospheric ozone depletion both generate poleward expansion of the Hadley circulation, they have nearly opposite influences on the strength. Increasing GHGs lead to

weakening of the Hadley circulation, whereas ozone depletion causes strengthening of the Hadley circulation. Third, while Allen et al. (2012, 2014) showed that anthropogenic aerosol forcing causes widening of the Hadley circulation, CMIP5 simulations demonstrate insignificant changes in both the width and strength of the Hadley circulations by anthropogenic aerosols.

Acknowledgments Y. Hu and L. Tao are supported by the National Natural Science Foundation of China (NSFC) under Grants 41375072 and 41025018. J. Liu is supported by NSFC (41176169). We thank J. Yang, Y. Ling and W. Kong for their great helps in improving the early draft. We acknowledge the World Climate Research Programme's Working Group on Coupled Modeling, which has coordinated CMIP5 simulations, and we thank the climate modeling groups (listed in Table 1 of this paper) for producing and making available their model output. For CMIP the U.S. Department of Energy's Program for Climate Model Diagnosis and Intercomparison provides coordinating support and led development of software infrastructure in partnership with the Global Organization for Earth System Science Portals.

References

Allen RJ, Sherwood SC, Norris JR, Zender CS (2012) Recent Northern Hemisphere tropical expansion primarily driven by black carbon and tropospheric ozone. Nature 485:350–354. doi:10.1038/nature11097

Allen RJ, Norris JR, Kovilakam M (2014) Influence of anthropogenic aerosols and the Pacific decadal oscillation on tropical belt width. Nat Geosci 7:270–274. doi:10.1038/NGEO2091

Archer CL, Caldeira K (2008) Historical trends in the jet streams. Geophys Res Lett 35:L08803. doi:10.1029/2008gl033614

Bindoff NL, Stott PA, AchutaRao KM, Allen MR, Gillett N, Gutzler D, Hansingo K, Hegerl G, Hu Y, Jain S, Mokhov I, Overland J, Perlwitz J, Sebbari R, Zhang X (2013) Detection and Attribution of Climate Change: from Global to Regional. In: Stocker TF, Qin D, Plattner G-K, Tignor M, Allen SK, Boschung J, Nauels A, Xia Y, Bex V, Midgley PM (eds) Climate change 2013: the physical science basis. Contribution of working group I to the fifth assessment report of the intergovernmental panel on climate change. Cambridge University Press, Cambridge, pp 867–952

Bond TC, Bhardwaj E, Dong R, Jogani R, Jung S, Roden C, Streets DG, Trautmann NM (2007) Historical emissions of black and organic carbon aerosol from energy-related combustion, 1850–2000. Global Biogeochem Cycles 21:1–16. doi:10.1029/2006GB002840

Cai W, Cowan T (2013) Southeast Australia autumn rainfall reduction: a climate-change-induced poleward shift of ocean-atmosphere circulation. J Clim 26:189–205. doi:10.1175/JCLI-D-12-00035.1

Cai W, Cowan T, Thatcher M (2012) Rainfall reductions over Southern Hemisphere semi-arid regions: the role of subtropical dry zone expansion. Sci Rep. doi:10.1038/srep00702

Chen G, Held IM (2007) Phase speed spectra and the recent poleward shift of Southern Hemisphere surface westerlies. Geophys Res Lett 34:L21805. doi:10.1029/2007gl031200

Cionni I, Eyring V, Lamarque JF, Randel WJ, Stevenson DS, Wu F, Bodeker GE, Shepherd TG, Shindell DT, Waugh DW (2011) Ozone database in support of CMIP5 simulations: results and corresponding radiative forcing. Atmos Chem Phys 11:11267–11292. doi:10.5194/acp-11-11267-2011

Davis SM, Rosenlof KH (2012) A multi-diagnostic intercomparison of tropical width time series using reanalyses and satellite observations. J Clim 25:1061–1078. doi:10.1175/JCLI-D-11-00127.1

Eyring V, Arblaster JM, Cionni I, Sedláček J, Perlwitz J, Young PJ, Bekki S, Bergmann D, Cameron-Smith P, Collins WJ, Faluvegi G, Gottschaldt K-D, Horowitz LW, Kinnison DE, Lamarque J-F, Marsh DR, Saint-Martin D, Shindell DT, Sudo K, Szopa S, Watanabe S (2013) Long-term ozone changes and associated climate impacts in CMIP5 simulations. J Geophys Res Atmos 118:5029–5060. doi:10.1002/jgrd.50316

Frierson DMW, Lu J, Chen G (2007) Width of the Hadley cell in simple and comprehensive general circulation models. Geophys Res Lett 34:L18804. doi:10.1029/2007gl031115

Fu Q, Johanson CM, Wallace JM, Reichler T (2006) Enhanced mid-latitude tropospheric warming in satellite measurements. Science 312:1179. doi:10.1126/science.1125566

Fu R, Yin L, Li W, Arias PA, Dickinson RE, Huang L, Chakrabortty S, Fernandes K, Liebmann B, Fisher R, Myneni RB (2013) Increased dry-season length over southern Amazonia in recent decades and its implication for future climate projection. Proc Natl Acad Sci 110:18110–18115. doi:10.1073/pnas.1302584110

Gettelman A, Hoor P, Pan LL, Randel WJ, Hegglin MI, Birner T (2011) The extratropical upper troposphere and lower stratosphere. Rev Geophys 49:RG3003. doi:10.1029/2011RG000355

Hartmann DL, Klein Tank AMG, Rusticucci M, Alexander LV, Brönnimann S, Charabi Y, Dentener FJ, Dlugokencky EJ, Easterling DR, Kaplan A, Soden BJ, Thorne PW, Wild M, Zhai PM (2013) Observations: Atmosphere and Surface. In: Stocker TF, Qin D, Plattner G-K, Tignor M, Allen SK, Boschung J, Nauels A, Xia Y, Bex V, Midgley PM (eds) Climate change 2013: The physical science basis. Contribution of working group I to the fifth assessment report of the intergovernmental panel on climate change. Cambridge University Press, Cambridge, pp 159–254

Hu Y, Fu Q (2007) Observed poleward expansion of the Hadley circulation since 1979. Atmos Chem Phys 7:5229–5236

Hu Y, Zhou C (2010) Decadal changes in the Hadley circulation. In: Oh JH (ed) Advances in Geosciences, vol 10. World Scientific Publishing Company, Singapore, p 250

Hu Y, Zhou C, Liu J (2011) Observational evidence for poleward expansion of the Hadley circulation. Adv Atmos Sci 28:33–44. doi:10.1007/s00376-010-0032-1

Hu Y, Tao L, Liu J (2013) Poleward expansion of the Hadley circulation in CMIP5 simulations. Adv Atmos Sci 30:790–795. doi:10.1007/s00376-012-2187-4

Hudson RD (2012) Measurements of the movement of the jet streams at mid-latitudes, in the Northern and Southern Hemispheres, 1979 to 2010. Atmos Chem Phys 12:7797–7808. doi:10.5194/acp-12-7797-2012

Hudson RD, Andrade MF, Follette MB, Frolov AD (2006) The total ozone field separated into meteorological regimes—part II: northern Hemisphere mid-latitude total ozone trends. Atmos Chem Phys 6:5183–5191. doi:10.5194/acp-6-5183-2006

Johanson CM, Fu Q (2009) Hadley cell widening: model simulations versus observations. J Clim 22:2713–2725. doi:10.1175/2008jcli2620.1

Kang SM, Polvani LM, Fyfe JC, Sigmond M (2011) Impact of polar ozone depletion on subtropical precipitation. Science 332:951–954. doi:10.1126/science.1202131

Lamarque J-F, Kyle GP, Meinshausen M, Riahi K, Smith SJ, Van Vuuren DP, Conley AJ, Vitt F (2011) Global and regional evolution of short-lived radiatively-active gases and aerosols in the representative concentration pathways. Clim Change 109:191–212. doi:10.1007/s10584-011-0155-0

Lu J, Vecchi GA, Reichler T (2007) Expansion of the Hadley cell under global warming. Geophys Res Lett 34:L06805. doi:10.1029/2006gl028443

Lu J, Deser C, Reichler T (2009) Cause of the widening of the tropical belt since 1958. Geophys Res Lett 36:L03803. doi:10.1029/2008gl036076

Lucas C, Timbal B, Nguyen H (2013) The expanding tropics: a critical assessment of the observational and modeling studies. Wiley Interdiscip Rev Clim Chang. doi:10.1002/wcc.251

Min S-K, Son S-W (2013) Multimodel attribution of the Southern Hemisphere Hadley cell widening: major role of ozone depletion. J Geophys Res Atmos 118:3007–3015. doi:10.1002/jgrd.50232

Moss RH, Edmonds JA, Hibbard KA, Manning MR, Rose SK, Van Vuuren DP, Carter TR, Emori S, Kainuma M, Kram T, Meehl GA, Mitchell JFB, Nakicenovic N, Riahi K, Smith SJ, Stouffer RJ, Thomson AM, Weyant JP, Wilbanks TJ (2010) The next generation of scenarios for climate change research and assessment. Nature 463:747–756. doi:10.1038/nature08823

Polvani LM, Previdi M, Deser C (2011a) Large cancellation, due to ozone recovery, of future Southern Hemisphere atmospheric circulation trends. Geophys Res Lett 38:L04707. doi:10.1029/2011GL046712

Polvani LM, Waugh DW, Correa GJP, Son S-W (2011b) Stratospheric ozone depletion: the main driver of twentieth-century atmospheric circulation changes in the Southern Hemisphere. J Clim 24:795–812. doi:10.1175/2010JCLI3772.1

Schneider T, Gorman PAO, Levine XJ, O'Gorman PA (2010) Water vapor and the dynamics of climate changes. Rev Geophys 48:RG3001. doi:10.1029/2009rg000302

Seidel DJ, Randel WJ (2007) Recent widening of the tropical belt: evidence from tropopause observations. J Geophys Res 112:D20113. doi:10.1029/2007jd008861

Seidel DJ, Fu Q, Randel WJ, Reichler TJ (2008) Widening of the tropical belt in a changing climate. Nat Geosci 1:21–24. doi:10.1038/ngeo.2007.38

Son S-W, Polvani LM, Waugh DW, Akiyoshi H, Garcia R, Kinnison D, Pawson S, Rozanov E, Shepherd TG, Shibata K (2008) The impact of stratospheric ozone recovery on the Southern Hemisphere westerly jet. Science 320:1486–1489. doi:10.1126/science.1155939

Son S-W, Polvani LM, Waugh DW, Birner T, Akiyoshi H, Garcia RR, Gettelman A, Plummer DA, Rozanov E (2009) The impact of stratospheric ozone recovery on tropopause height trends. J Clim 22:429–445. doi:10.1175/2008JCLI2215.1

Son S-W, Gerber EP, Perlwitz J, Polvani LM, Gillett NP, Seo K-H, Eyring V, Shepherd TG, Waugh D, Akiyoshi H, Austin J, Baumgaertner A, Bekki S, Braesicke P, Brühl C, Butchart N, Chipperfield MP, Cugnet D, Dameris M, Dhomse S, Frith S, Garny H, Garcia R, Hardiman SC, Jöckel P, Lamarque JF, Mancini E, Marchand M, Michou M, Nakamura T, Morgenstern O, Pitari G, Plummer DA, Pyle J, Rozanov E, Scinocca JF, Shibata K, Smale D, Teyssèdre H, Tian W, Yamashita Y (2010) Impact of stratospheric ozone on Southern Hemisphere circulation change: A multimodel assessment. J Geophys Res Atmos 115:D00M07. doi:10.1029/2010jd01427

Stachnik JP, Schumacher C (2011) A comparison of the Hadley circulation in modern reanalyses. J Geophys Res 116:D22102. doi:10.1029/2011jd016677

Sun L, Chen G, Lu J (2013) Sensitivities and mechanisms of the zonal mean atmospheric circulation response to tropical warming. J Atmos Sci 70:2487–2504. doi:10.1175/JAS-D-12-0298.1

Tandon NF, Gerber EP, Sobel AH, Polvani LM (2013) Understanding Hadley cell expansion versus contraction: insights from simplified models and implications for recent observations. J Clim 26:4304–4321. doi:10.1175/jcli-d-12-00598.1

Taylor GT, Muller-Karger FE, Thunell RC, Scranton MI, Astor Y, Varela R, Ghinaglia LT, Lorenzoni L, Fanning KA, Hameed S, Doherty O (2012a) Ecosystem responses in the southern Caribbean Sea to global climate change. Proc Natl Acad Sci 109:19315–19320. doi:10.1073/pnas.1207514109

Taylor KE, Stouffer RJ, Meehl GA (2012b) An overview of CMIP5 and the experiment design. Bull Am Meteorol Soc 93:485–498. doi:10.1175/bams-d-11-00094.1

Wilcox LJ, Highwood EJ, Dunstone NJ (2013) The influence of anthropogenic aerosol on multi-decadal variations of historical global climate. Environ Res Lett 8:024033. doi:10.1088/1748-9326/8/2/024033